Binding of inhibitory fatty acids is responsible for the enhancement of UDP-glucuronosyltransferase 2B7 (UGT2B7) activity by albumin: Implications for *in vitro-in vivo* extrapolation.

Andrew Rowland, Paraskevi Gaganis, David J Elliot, Peter I Mackenzie, Kathleen M Knights and John O Miners

Department of Clinical Pharmacology, Flinders University and Flinders Medical Centre, Bedford Park, Adelaide, Australia.

1

JPET #118216

Running Title: Mechanism of the albumin effect on UGT2B7

Corresponding author:

Professor John Miners

Department of Clinical Pharmacology

Flinders Medical Centre

Bedford Park

SA 5042

Australia

telephone   61-8-82044131

fax   61-8-82045114

email   john.miners@flinders.edu.au

Manuscript details:

Number of text pages (including references and legends) – 38

Number of tables – 5

Number of figures – 5

Number of references – 40

Abstract – 250 words

Introduction – 714 words

Discussion – 1482 words

Abbreviations:

AZT, zidovudine; BSA, bovine serum albumin; BSA-FAF, essentially fatty acid free BSA; BSA-GF, essentially globulin free BSA; BSA-FAFGF, essentially fatty acid and globulin free BSA; CYP, cytochrome P450; FA, fatty acid; FAME, fatty acid methyl ester; HLM, human liver microsomes; HSA, human serum albumin; HSA-FAF, essentially fatty acid free HSA; HSA-GF, essentially globulin free HSA; HSA-FAFGF, essentially fatty acid free and globulin free HSA; 4MU, 4-methylumbelliferone; 4MUG, 4-methylumbelliferone-β-D-glucuronide; UDPGA, UDP-glucuronic acid, UGT, UDP-glucuronosyltransferase.

ABSTRACT

Studies were performed to elucidate the mechanism responsible for the reduction in K_m values of UGT2B7 substrates observed for incubations conducted in the presence of albumin. Addition of BSA and fatty acid free HSA (HSA-FAF), but not 'crude' HSA, resulted in an approximate 90% reduction in the K_m values for the glucuronidation of AZT by HLM and UGT2B7 and a 50% to 75% reduction in the S_{50} for 4-methylumbelliferone (4MU) glucuronidation by UGT2B7, without affecting V_{max}. Oleic, linoleic and arachidonic acids were shown to be the most abundant unsaturated long chain fatty acids present in 'crude' HSA and in the membranes of HLM and HEK293 cells, and it was demonstrated that these and other unsaturated long chain fatty acids were UGT2B7 substrates. Glucuronides with R_f values corresponding to the glucuronides of linoleic and arachidonic acid were detected when HLM and HEK293 cell lysate were incubated with radiolabelled cofactor, and the intensity of the bands was modulated by the presence of 'crude' HSA (increased) and BSA or HSA-FAF (decreased). Oleic, linoleic and arachidonic acid inhibited AZT and 4MU glucuronidation by HLM and/or UGT2B7, due to an increase in K_m/S_{50} without a change in V_{max}. Addition of BSA and HSA-FAF reversed the inhibition. Similarly, co-expression of UGT2B7 and HSA in HEK293 cells reduced the K_m/S_{50} values of these substrates. It is postulated that BSA and HSA–FAF sequester inhibitory fatty acids released during incubations, and the apparent high K_m values observed for UGT2B7 substrates arise from the presence of these endogenous inhibitors.

3

INTRODUCTION

In vitro approaches for the prediction of drug pharmacokinetic parameters *in vivo* (*in vitro – in vivo* extrapolation) have attracted widespread interest in recent years, particularly for the assessment of metabolic stability in preclinical drug development (Ward 2005). In this regard, an intrinsic clearance (CL_{int}) for a metabolic pathway determined using human liver microsomes (HLM), fresh or cryopreserved human hepatocytes, or recombinant cytochrome P450 (CYP) enzymes, may be extrapolated to a whole liver value using appropriate scaling factors (Houston 1994; Griffin and Houston 2004; Miners *et al.* 2004; Proctor *et al.* 2004). Hepatic clearance (CL_H) and extraction ratio are then estimated using a mathematical expression, typically the 'well stirred model', that relates this parameter to CL_{int}, liver blood flow (Q_H) and the fraction of drug unbound in blood ($f_{u,b}$) (Houston 1994; Iwatsubo *et al.* 1997, Ito *et al.* 1998). It is similarly possible to predict the magnitude of an inhibitory drug-drug interaction *in vivo* based on measurement of an inhibitor constant (K_i) (Ito *et al.* 1998; von Moltke *et al.* 1998; Ito and Houston 2004; Wienkers and Heath 2005).

Despite the widespread use of *in vitro – in vivo* extrapolation, the use of HLM as the enzyme source generally results in underestimation of the *in vivo* CL_H (Ito and Houston 2005). For drugs eliminated by glucuronidation, *in vivo* CL_H is typically under-predicted by an order of magnitude using physiologically based scaling factors (Mistry and Houston 1987; Boase and Miners 2002; Soars *et al.* 2002; Engtrakul *et al.* 2005; Riley *et al.* 2005). Prediction accuracy is improved with the use of fresh or cryopreserved human hepatocytes (Soars *et al.* 2002; McGinnity *et al.* 2005), but the bias for under-prediction remains (Ito and Houston 2005; Miners *et al.* 2006). Similar observations have been reported in studies investigating inhibition of drug glucuronidation with HLM as the enzyme source; experimental K_i values resulted in

4

under-prediction of the magnitude of inhibitory interactions involving glucuronidated drugs *in vivo* (Rowland *et* al. 2006; Uchaipichat *et al.* 2006).

It has been demonstrated previously that addition of bovine serum albumin (BSA) to human liver microsomal incubations decreases the K_m and increases the *in vitro* CL_{int} for drugs metabolized by CYP2C9 (Ludden *et al.* 1997; Carlile *et al.* 1999; Tang *et al.* 2002; Wang *et al.* 2002; Zhou *et al.* 2004). Improved predictivity of *in vivo* CL_{int} values occurred for experiments conducted in the presence of BSA. Subsequent studies conducted in this laboratory demonstrated that the addition of BSA (2%) to incubations of HLM and recombinant UGT2B7 increased the *in vitro* CL_{int} for lamotrigine and zidovudine (AZT) glucuronidation 7- to 10-fold (Rowland *et al.* 2006; Uchaipichat *et al.* 2006). Moreover, the addition of BSA reduced the K_i values for valproic acid inhibition of lamotrigine glucuronidation and fluconazole inhibition of AZT glucuronidation by almost an order of magnitude, such that the magnitude of these interactions *in vivo* were predicted correctly from *in vitro* inhibition constants.

Despite the greatly improved predictivity of *in vitro – in vivo* clearance extrapolation for microsomal incubations conducted in the presence of BSA, the mechanism of the 'albumin' effect remains unknown. The 'mopping up' of endogenous inhibitors present in microsomal incubations or altered protein (CYP or UGT) conformation have been proposed (Tang *et al.* 2002; Rowland *et al* 2006; Uchaipichat *et al.* 2006), but neither have been investigated in a systematic manner. Here we compared the effects of BSA and human serum albumin (HSA) in their 'crude', fatty acid free (FAF), globulin free (GF) and fatty acid and globulin free (FAFGF) forms on the glucuronidation of AZT by HLM and recombinant UGT2B7 (expressed in HEK293 cells) and on 4-methylumbelliferone (4-MU) glucuronidation by UGT2B7. The glucuronidation of AZT, a selective substrate for UGT2B7, follows Michaelis Menten kinetics (Boase and Miners 2002; Court *et al.* 2003) whereas 4-MU glucuronidation by recombinant

5

UGT2B7 exhibits sigmoidal kinetics characteristic of autoactivation (Uchaipichat *et al.* 2004). (Since 4-MU is a non-selective UGT substrate, 4-MU glucuronidation was not investigated with HLM as the enzyme source.) Results obtained with the albumin preparations and subsequent inhibition experiments demonstrated that unsaturated long chain fatty acids present in the microsomal and HEK293 cell lysate preparations act as potent competitive inhibitors of AZT and 4-MU glucuronidation, and sequestration of fatty acids is responsible for the higher binding affinities observed in the presence of certain albumin preparations.

MATERIALS AND METHODS

Materials

Alamethicin (from *Trichoderma viride*), bovine serum albumin ('crude' BSA, product number A7906), essentially fatty acid free BSA (BSA-FAF; product number A6003), essentially globulin free BSA (BSA-GF; product number A3059), essentially fatty acid and globulin free BSA (BSA-FAFGF; product number A0281), human serum albumin ('crude' HSA; product number A9511), essentially fatty acid free HSA (HSA-FAF; product number A1887), essentially globulin free HSA (HSA-GF; product number A8753), essentially fatty acid and globulin free HSA (HSA-FAFGF; product number A3782), 4-methylumbelliferone (4MU), 4-methylumbelliferone β-D-glucuronide (4MUG), fatty acids (as the free acid), UDP-glucuronic acid (UDPGA, trisodium salt), [^{14}C]-UDPGA and zidovudine (AZT) were purchased from Sigma Aldrich (Sydney, Australia). (Albumin product numbers have been provided to allow details of each preparation, including method of isolation, to be accessed from the supplier's web-site.) Human serum albumin TrueClone cDNA (reference sequence NM_000477.3, length 2110bp) was purchased from Origene (Rockville, USA). Solvents and other reagents were of analytical reagent grade.

Human liver microsomes and expression of UGT2B7

Pooled human liver microsomes were prepared by mixing equal protein amounts from five human livers (H7, 44yo female; H10, 67yo female; H12, 66yo male; H29 45yo male; and H40, 54yo female), obtained from the human liver 'bank' of the Department of Clinical Pharmacology of Flinders University. Approval for the use of human liver tissue in xenobiotic metabolism studies was obtained from both the Clinical Investigation Committee of Flinders Medical Centre and from the donors' next-of-kin.

Human liver microsomes (HLM) were prepared by differential centrifugation, as described by Bowalgaha *et al.* (2005).

A cDNA encoding UGT2B7 was stably expressed in a human embryonic kidney cell line (HEK293), as described previously (Stone *et al.* 2003). Cell lines were transfected with the UGT2B7 cDNA cloned into the expression vector pEF-IRES-puro6. Transfected cells were incubated in Dulbecco's modified Eagle's medium, which contained puromycin (1mg/L) and fetal calf serum (10%) in a humidified incubator at 37ºC with an atmosphere of 5% CO_2. Following growth to at least 80% confluency, cells were harvested and washed with phosphate buffered saline (0.1M, pH 7.4). Cells were subsequently lysed by sonication using a Heat Systems-Ultrasonics sonicator set at microtip limit of four, with four 1sec 'bursts', separated by 3 min with cooling on ice. Lysed samples were centrifuged at 12000g for 1 min at 4ºC, and the supernatant fraction was removed and stored at –80ºC until use. Expression of UGT2B7 protein was demonstrated by immunoblotting with a non-selective UGT antibody (raised against purified mouse Ugt) according to Uchaipichat *et al.* (2004) and activity measurement (see below).

UGT2B7 and HSA cDNAs, each cloned into the expression vector pEF-IRES-puro6, were co-transfected in HEK293 cells following the procedure described above for UGT2B7. Transfected cells were treated as detailed for stably expressed UGT2B7. Expression of the HSA protein was quantified by immunoblotting (see below).

Immunoblotting of HSA

HEK293 cell lysate protein (20µg) was subjected to 10% SDS PAGE. Proteins were rectilinearly transferred onto nitrocellulose, and probed with goat anti-HSA primary antiserum (1:1000 dilution; Sigma Genosys, Sydney, Australia) and rabbit anti-goat

8

IgG (1:1000 dilution; H+L-HRP) as the secondary antibody (Southern Biotechnology Associates Inc., Birmingham, AL). Membrane-bound peptides conjugated with HRP were detected by chemiluminescence (Roche Diagnostics, Mannheim, Germany) and subsequently exposed to Omat autoradiographic film (Kodak). Autoradiographs were processed manually with AGFA developer, fixer and replenisher reagents. Quantification of HSA expression was achieved by comparison of band intensity to those of a standard curve constructed using known concentrations of HSA.

AZT glucuronidation assay

Incubations, in a total volume of 200µl, contained phosphate buffer (0.1M, pH 7.4), $MgCl_2$ (4mM), HLM (0.1mg), albumin (0-4%), and AZT (25-4000µM). HLM were fully activated by the addition of the pore-forming polypeptide alamethicin (50µg/mg protein) with incubation on ice for 30 min (Boase and Miners, 2002). Following a 5 min pre-incubation, reactions were initiated by the addition of UDPGA (5mM). Incubations were performed at 37ºC in a shaking water bath for 60 min. Reactions were terminated by the addition of perchloric acid (6µl, 70% v/v). Samples were subsequently centrifuged at 4000g for 10 min, and a 30µl aliquot of the supernatant fraction was injected directly into the HPLC column. For reactions performed using recombinant UGT2B7, incubation mixtures contained HEK293 cell lysate (0.15mg) in place of HLM protein, and the incubation time was increased to 90 min. Under the reaction conditions employed, AZT glucuronidation was linear with respect to incubation time to 120 min, and protein concentration to 1.75mg/ml for both HLM and HEK293 cell lysate as the enzyme source. AZT glucuronidation by lysate from untransfected HEK293 cells was not detectable.

Quantification of GAZT formation

9

HPLC was performed using an Agilent 1100 series instrument (Agilent Technologies, Sydney, Australia) fitted with a Waters NovaPak C18 analytical column (150 x 3.9mm 4µm, Waters, Sydney, Australia). GAZT was separated with a mobile phase containing 10mM triethylamine (pH adjusted to 2.5 with perchloric acid) and 10% acetonitrile, at a flow rate of 1ml/min. Column eluant was monitored by UV absorbance at 267nm. Retention times for GAZT and AZT were 4.0 and 6.1 min, respectively. GAZT formation was quantified by comparison of peak areas to those of an AZT standard curve prepared over the concentration range 1 – 25µM. Overall within day assay reproducibility was assessed by measuring GAZT formation in 8 separate incubations of the same batch of pooled HLM. Coefficients of variation were 3.8% and 3.1% for the AZT concentrations of 25µM and 4000µM, respectively.

4MU glucuronidation assay

Incubations, in a total volume of 200µl, contained phosphate buffer (0.1M, pH 7.4), $MgCl_2$ (4mM), albumin (0-2%), HEK293 cell lysate expressing UGT2B7 (0.2mg/ml) and 4MU (25-1500µM). Following a 5 min pre-incubation, reactions were initiated by the addition of UDPGA (5mM). Incubations were performed at 37ºC in a shaking water bath for 90 min. Reactions were terminated by the addition of perchloric acid (6µl, 70% v/v). Samples were subsequently centrifuged at 4000g for 10 min, and a 25µl aliquot of the supernatant fraction was injected directly into the HPLC column. 4MU β-D-glucuronidation by lysate from untransfected HEK293 cells was not detectable.

Quantification of 4MUG formation

The HPLC instrument and column were as described for the measurement of GAZT. 4MUG was separated by gradient elution at a flow rate of 1ml/min. Initial conditions

were 96% 10mM triethylamine buffer containing perchloric acid (pH2.5) and 10%
acetonitrile (mobile phase A) and 4% acetonitrile (mobile phase B). These conditions
were held for 3 min, then the proportion of mobile phase B was increased to 30% over
0.1min, and held for 1min. Column eluant was monitored by UV absorbance at
316nm. Retention times for 4MUG and 4MU were 3.6 and 5.8min, respectively. 4MUG
formation was quantified by comparison of peak areas to those of an authentic 4MUG
standard curve prepared over the concentration range 1 – 10µM. Overall within day
assay reproducibility was assessed by measuring 4MUG formation in 8 separate
incubations of the same batch of expressed UGT2B7. Coefficients of variation were
4.3% and 2.6% for 4MU concentrations of 50µM and 1500µM, respectively.

Fatty acid glucuronidation assay

The glucuronidation of the fatty acids listed in legend to Figure 3 was demonstrated
using a radiometric thin layer chromatography method. Incubations (100µl) contained
phosphate buffer (0.1 M, pH 6.8), $MgCl_2$ (4mM), HEK293 cell lysate expressing
UGT2B7 (1.7mg/ml), UDPGA [total concentration 50µM, consisting of [^{14}C]-UDPGA
(0.1µCi, 5µl) and non-labelled UDPGA (47µM)], and fatty acid (100µM). Fatty acids
were added as solutions in ethanol such that the final concentration of solvent in
incubations was 1%v/v. This concentration of ethanol has been demonstrated
previously to cause <20% inhibition of recombinant UGT2B7 activity (Uchaipichat *et
al.* 2004). Weakly acidic (pH 6.8) conditions were employed to minimize hydrolysis of
the fatty acid acyl glucuronides formed during the course of an incubation. Incubations
were performed at 37ºC in a shaking water bath for 120min. For experiments
demonstrating the glucuronidation of fatty acids present in preparations of HLM and
recombinant UGT2B7, incubation mixtures contained albumin (0 - 2%), HLM or cell
lysate expressing UGT2B7 (2mg/ml) and UDPGA (5mM, containing [^{14}C]-UDPGA
0.2µCi, 10µL). Arachidonic and linoleic acids were included as positive controls.

Separation of fatty acid glucuronides was achieved by development of TLC plates in butan-1-ol - acetic acid - 35% ammonia - water (35:25:9:0.7:30.3). Following development, plates were air-dried overnight and exposed in Storage Phosphor Screen Cassettes (Molecular Dynamics Inc., CA, USA) for up to ten days. Quantitative densitometry of glucuronides was undertaken using a scanning laser Phosphorimager and associated ImageQuant software (Molecular Dynamics Inc.) with reference to a standard curve constructed using known concentrations of [^{14}C]-UDPGA.

Quantification of the fatty acid content of HLM, BSA, HSA and HSA-FAF

The fatty acid contents of HLM (1mg/ml), BSA (2%), HSA (2%) and HSA-FAF (2%) were determined by gas-liquid chromatography using a modification of the method of Folch *et al*. (1956). Briefly, triheptadecanoin (C17:0; the internal standard) was added to a known volume of sample and lipids were extracted with 2:l chloroform:methanol (5ml). Samples were transesterified with methanol (containing 1% H_2SO_4) at 70°C for 3hr. Fatty acid methyl esters (FAME) were extracted with water and n-heptane for analysis by gas-liquid chromatography. FAMEs were separated and quantified using a Hewlett-Packard 6890 gas chromatograph equipped with a 50m x 0.32mm capillary column coated with BPX-70 (0.25µm film thickness, SGE Pty Ltd, Victoria, Australia). Injector and detector (flame ionisation) temperatures were set at 250 and 300°C, respectively, while the initial oven temperature of 140°C was programmed to rise to 220°C at a rate of 5°C/min. Helium was used as the carrier gas at a velocity of 35cm/sec. FAMEs were identified based on the retention times of authentic lipid standards (GLC-463, Nuchek Prep Inc. Elysian, MN) and quantified by comparison to the internal standard using ChemStation software (Agilent, CA).

Binding of AZT and 4MU to albumin, HLM and HEK293 cell lysate

Binding of AZT and 4MU to HLM, HEK293 cell lysate, albumin (0.1, 0.5, 1 and 2%) and mixtures of albumin with each enzyme source was measured by an equilibrium dialysis method according to McLure *et al.* (2000). Binding measurements were performed using a Dianorm equilibrium dialysis apparatus that comprised Teflon™ dialysis cells (capacity of 1200µl per side) separated into two compartments with Sigma Aldrich dialysis membrane (molecular mass cut off 12kDa). One side of the dialysis cell was loaded with 1ml of a solution of AZT (100 to 2000µM) or 4MU (50 to 1000µM) in phosphate buffer (0.1M, pH 7.4). The other compartment was loaded with 1ml of either a suspension of HLM in phosphate buffer (0.1M, pH 7.4), HEK293 cell lysate in phosphate buffer (0.1M, pH 7.4), albumin (0.1, 0.25, 0.5, 1 and 2%) in phosphate buffer (0.1M pH 7.4), or a combination of albumin with each enzyme source in phosphate buffer (0.1M, pH 7.4). The dialysis cell assembly was immersed in a water bath maintained at 37ºC and rotated at 12rpm for 4hr. Control experiments were also performed with phosphate buffer or albumin on both sides of the dialysis cells at low and high concentrations of all substrates to ensure that equilibrium was attained. A 200µl aliquot was collected from each compartment, treated with ice-cold methanol containing 8% glacial acetic acid (200µl), and cooled on ice. Samples were subsequently centrifuged at 4000g for 10 min at 10ºC and an aliquot of the supernatant fraction (5µl) was analysed by HPLC.

Quantification of AZT and 4MU binding

The HPLC instrument and column used was as described for the measurement of AZT and 4MU glucuronide formation. Separation of AZT was achieved using a 65:35 mixture of mobile phases A and B, as utilized for the GAZT assay. The mobile phase flow rate was 1.0ml/min. Column eluant was monitored at 267nm. The retention time

for AZT under these conditions was 2.6 min. 4MU separation was achieved using a

70:30 mixture of mobile phases A and B (as described previously) at a flow rate of

1.0ml/min. Column eluant was monitored at 316nm. The retention time for 4MU was

2.9min. AZT and 4MU concentrations in dialysis samples were determined by

comparison of peak areas to those of a standard curve, in the respective

concentration ranges 100 to 2000μM and 10 to 1000μM. Within day assay variability

was assessed by measuring AZT (100 and 2000μM) or 4MU (50 and 1000μM) (n=5

for each concentration) in samples containing phosphate buffer (0.1M, pH 7.4) or BSA

in phosphate buffer (0.1M, pH 7.4). Coefficients of variation were less than 5% in all

cases.

Data analysis

Kinetic data are presented as mean values derived from experiments with pooled

HLM (4 replicates) and duplicate experiments with recombinant UGT2B7. Kinetic

constants (K_m and V_{max}) for AZT glucuronidation by HLM and recombinant UGT2B7 in

the presence and absence of albumin were generated by fitting experimental data to

the Michaelis-Menten equation (Uchaipichat *et al*. 2006). Kinetic constants for 4MU β-

D-glucuronidation by recombinant UGT2B7, a reaction which exhibits homotropic

positive cooperativity (or 'autoactivation), in the presence and absence of albumin

were obtained by fitting data to the Hill equation to obtain estimates of S_{50}, V_{max} and n

(the Hill coefficient) (Uchaipichat *et al*. 2004). In all cases, fitting was based on

unbound substrate concentrations in incubations and performed with EnzFitter

(Biosoft, Cambridge, UK). Intrinsic clearances (CL_{int}) for AZT glucuronidation by HLM

and UGT2B7 were determined as V_{max}/K_m. Maximal clearance (CL_{max}) for 4MU

glucuronidation by UGT2B7, which exhibits autoactivation, was calculated according

to Houston and Kenworthy (2000), where n is the Hill coefficient (see above):

JPET #118216

$$CL_{max} = \frac{V_{max}}{S_{50}} \times \frac{(n-1)}{n(n-1)^{1/n}} \quad \text{———} \quad \text{equation 1}$$

Where appropriate, statistical analysis (univariate General Linear Model, with Tukey post hoc analysis) was performed using SPSS for Windows, rel. 12.0.1, 2003 (SPSS Inc., Chicago). Values of p less than 0.05 were considered significant.

RESULTS

Binding of AZT and 4MU to albumin

The binding of AZT and 4MU to incubation components, including various forms of albumin, was calculated as the concentration of drug in the buffer compartment divided by the concentration of drug in the protein compartment and expressed as the fraction unbound in incubations ($f_{u,inc}$). Binding of AZT to pooled HLM, HEK293 cell lysate and combinations of each enzyme source with the various types of albumin (0.1-2%) was negligible (<5%) across the AZT concentration range investigated (10 to 2000μM). Similarly, 4MU binding to HEK293 cell lysate was negligible (<5%) across the concentration range investigated. However, 4MU bound significantly to all forms of albumin. 4MU binding was independent of concentration over the range investigated (50 to 1500μM), but varied with albumin concentration and form. The mean $f_{u,inc}$ value for 4MU binding to BSA ranged from 0.89 (0.1% BSA) to 0.27 (2% BSA). Significant binding of 4MU to HSA was also observed. Mean $f_{u,inc}$ values for 4MU binding to mixtures of HSA and HEK293 cell lysate ranged from 0.79 (0.1% HSA) to 0.14 (2% HSA). There was a slight increase in the binding of 4MU to HSA-FAF; $f_{u,inc}$ values ranged from 0.76 (0.1% HSA-FAF) to 0.09 (2% HSA-FAF). Where observed, the concentration of 4MU present in incubation mixtures was corrected for binding in the calculation of kinetic parameters.

Effect of albumin on AZT glucuronidation by HLM and recombinant UGT2B7

Kinetic data for zidovudine glucuronide (GAZT) formation by human liver microsomal and recombinant UGT2B7, in the presence and absence of albumin, was well modelled by the expression for the Michaelis-Menten equation. Kinetic parameters for AZT glucuronidation in the presence of the various forms of BSA and HSA are shown

16

in Tables 1 and 2, respectively. The mean K_m and V_{max} values for AZT glucuronidation by HLM and recombinant UGT2B7 in the absence of albumin were 1113μM and 738pmol/min.mg, and 439μM and 50pmol/min.mg, respectively. These values are similar to those reported in previous publications from this and other laboratories (Boase and Miners 2002; Court *et al.* 2003; Uchaipichat *et al.* 2006).

All forms of BSA (at concentrations ranging from 0.1 to 4%) increased the rate of AZT glucuronidation by both human liver microsomal and recombinant UGT2B7 (Figure 1). The activation of AZT glucuronidation plateaued at concentrations above 0.5% for all forms of BSA. Kinetic analysis at 0.5 and 2% BSA revealed that the enhanced rate of AZT glucuronidation occurred due to a decrease ($p < 0.05$) in the K_m for this pathway, without a significant effect on V_{max} (Table 1 and Figure 2). Crude (unmodified) HSA displayed a concentration-dependent and biphasic (activation and inhibition) interaction with human liver microsomal and recombinant UGT2B7 (Figure 1). The K_m for AZT glucuronidation was initially reduced for incubations performed in the presence of 0.1% HSA, while the addition of 2% HSA caused an increase in the K_m for AZT glucuronidation (Table 2 and Figure 2). In contrast, HSA-FAF increased (4- to 9- fold) the rate of AZT glucuronidation by HLM and recombinant UGT2B7 in a concentration dependent manner up to 0.5%, after which activity plateaued (Figure 1). Like the effect of BSA preparations, this was due to a decrease in K_m (Table 2 and Figure 2). HSA-GF and HSA-FAFGF also caused activation of human liver microsomal and recombinant UGT2B7 (Figure 1 and Table 2). However, the magnitude of the effect decreased with increasing concentrations of these albumin preparations.

Effect of albumin on 4MU glucuronidation by recombinant UGT2B7

17

Based on the data for AZT, the effects of BSA, HSA and HSA-FAF on 4MU glucuronidation by UGT2B7 were also investigated. The kinetics of 4-MU β-D-glucuronide (4MUG) formation by recombinant UGT2B7, in the presence and absence of albumin, were best described by the Hill equation, with a value of n>1, indicating positive cooperativity. Kinetic parameters for 4MU β-D-glucuronidation in the presence of albumin (BSA, HSA, and HSA-FAF) are shown in Table 3. The S_{50}, n and V_{max} values for 4MU β-D-glucuronidation by recombinant UGT2B7 in the absence of albumin were 462μM, 1.6 and 1065pmol/min/mg, respectively. These values are in agreement with previous reports for this reaction (Uchaipichat *et al.* 2004). BSA and HSA-FAF increased the rate of 4MU β-D-glucuronidation by recombinant UGT2B7 in a concentration dependant manner. The S_{50} for this pathway was reduced by 50% and 75% for BSA and HSA-FAF, respectively, without a significant effect on either n or V_{max} (Table 3). Crude HSA did not have a significant effect on any of the kinetic parameters for the glucuronidation of 4MU by recombinant UGT2B7 at any albumin concentration (up to 2%, Table 3).

Fatty acid content of HLM and albumin preparations

Table 4 details the concentrations of C16 to C20 series fatty acids present in HLM, HEK293 cell lysate, BSA, HSA and HSA-FAF preparations. The total concentration of fatty acid in HLM (1mg/ml), HEK293 cell lysate (1mg/ml), HSA (2%), BSA (2%) and HSA-FAF (2%) was 334, 28, 202, 28 and 35μM, respectively, of which unsaturated fatty acids made up 70, 58, 56, 36 and 58%, respectively. Of the fatty acids known to inhibit UGT2B7 (Tsoutsikos *et al.* 2004), oleic acid (C18:1n-9), linoleic acid (C18:2n-6) and arachidonic acid (C20:4n-6) were observed in the highest concentrations. The fatty acid content of HLM was comparable to values published previously (Waskell *et*

18

al. 1982; Kapitulnik *et al*. 1987), and approximately 10-fold higher than the fatty acid content of HEK293 cell lysate.

Fatty acid glucuronidation by UGT2B7

Selected saturated and unsaturated fatty acids identified in HLM and human albumin preparations were screened to determine whether they were glucuronidated by UGT2B7. Recombinant UGT2B7 glucuronidated all C14, C16, C18 and C20 saturated and unsaturated fatty acids screened (at an added concentration of 100μM; Figure 3). Rates of glucuronidation of the C18- series fatty acids increased with the degree of unsaturation; 21, 30, 36, 59 pmol/min.mg for C18:0, C18:1, C18:2 and C18:3, respectively. In contrast, with the exception of eicosenoic acid (C20:1), rates of UGT2B7 catalyzed glucuronidation of the C20- fatty acids decreased as the degree of unsaturation increased; 19, 27, 99, 82, 75, and 43 pmol/min.mg for C20:0, C20:1, C20:2, C20:3, C20:4 and C20:5, respectively. Like the C18 and C20 series, rates of glucuronidation of the saturated C14 (12 pmol/min.mg) and C16 (17 pmol/min.mg) fatty acids were lower than their respective monounsaturated derivatives (54 and 43 pmol/min.mg).

Formation of fatty acid glucuronides by preparations of HLM and HEK293 cell lysate

The formation of glucuronides of compounds present in (or released by) incubation mixtures of HLM and HEK293 cell lysate expressing UGT2B7, in the presence and absence of BSA and crude and fatty acid free forms of HSA, was determined in the absence of an exogenous substrate. For comparison, incubations were conducted with added linoleic acid (10μM), arachidonic acid (10μM) and 4MU (5μM; as a representative xenobiotic substrate.). Bands corresponding to the R_f values of the

arachidonic acid and linoleic acid glucuronides were detected by TLC for incubations conducted in the presence of HLM and ^{14}C-labelled UDPGA without albumin (Figure 4). Based on band intensity, the concentration of the putative fatty acid glucuronides present in the incubation of HLM was 0.4 µM. The intensity of bands was substantially lower using HEK293 cell lysate expressing UGT2B7; the lower band intensity precluded meaningful product quantification. Increasing concentrations of HSA (0.1 - 2%) in incubations with each enzyme source increased the intensity of these bands in a concentration dependent manner. For example, the concentration of fatty acid glucuronides present in the incubation of HLM with 'crude' HSA (2%) was 1.5 µM. In contrast, addition of BSA and HSA-FAF (0.1 and 2%) to incubations resulted in a concentration dependent reduction in the intensity of the bands, with essentially no product visible for incubations conducted in the presence of either form of albumin at an added concentration of 2% (Figure 4).

Inhibition of AZT and 4MU glucuronidation by fatty acids in the presence and absence of albumin.

Inhibition of AZT glucuronidation, at an added concentration of 400µM (the approximate K_m), by oleic acid (C18:1), linoleic acid (C18:2), arachidonic acid (C20:4) and a mixture comprising 40% C18:1, 40% C18:2 and 20% C20:4 was measured in the presence and absence of albumin preparations using recombinant UGT2B7 as the enzyme source. Each fatty acid caused between 25% and 60% inhibition when present at one twentieth of the concentration observed in HLM (see above) (Table 5). When added as a mixture, the fatty acids did not increase in the magnitude of inhibition above that observed for the most potent inhibitor (arachidonic acid). The presence of BSA (2%) or HSA-FAF (2%) in incubations reversed the inhibitory effects of the fatty acids (Table 5).

The effect a combination of fatty acids (totaling 7.5µM, comprising 3µM C18:1, 3µM C18:2 and 1.5µM C20:4) on the kinetics of AZT and 4MU glucuronidation by recombinant UGT2B7 was characterized in the presence and absence of BSA (2%). In the absence of BSA (2%), the combination of fatty acids caused a 3 fold- increase in the K_m for AZT glucuronidation by recombinant UGT2B7, from 439µM to 1342µM without a significant effect on V_{max} (56 versus 61pmol/min.mg). In the presence of BSA (2%), the combination of fatty acids had no effect on the kinetics of AZT glucuronidation by recombinant UGT2B7; respective K_m and V_{max} values in the presence of BSA were 53 and 50µM and 60 and 61pmol/min.mg, for experiments performed in the absence and presence of fatty acids. In the absence of BSA (2%), the combination of fatty acids caused a 50% increase in the S_{50} for 4MU glucuronidation by recombinant UGT2B7, from 462µM to 612µM without a significant effect on n or V_{max} (987 versus 972pmol/min.mg). In the presence of BSA (2%), the combination of fatty acids had no effect on the kinetics of 4MU glucuronidation by recombinant UGT2B7; respective S_{50}, n and V_{max} values in the presence of BSA were 227 and 238µM, 1.7 and 1.7, and 933 and 984pmol/min.mg, for experiments performed in the absence and presence of fatty acids.

AZT and 4MU glucuronidation by recombinant UGT2B7 co-expressed with HSA

The content of HSA, determined by immunoblotting, in HEK293 cell lysates co-expressing HSA and UGT2B7 was approximately 9nmol/mg (Figure 5); this corresponds to an HSA concentration of 0.6mg/ml (ie. 0.06%) in a 0.2ml incubation containing 1mg/ml of cell lysate. The kinetics of GAZT formation by recombinant UGT2B7 co-expressed with recombinant HSA were well modelled using the Michaelis-Menten equation, with K_m and V_{max} values of 212µM and 47pmol/min.mg, respectively. The K_m is approximately half that observed for this pathway in the absence of co-expressed recombinant HSA (439µM). In contrast, the V_{max} value

21

(47pmol/min.mg) for AZT glucuronidation in HEK293 cell lysates expressing both UGT2B7 and HSA was essentially identical to the value (50pmol/min.mg) for cells expressing UGT2B7 alone. The kinetics of 4MUG formation by recombinant UGT2B7 co-expressed with recombinant HSA were well modelled using the Hill equation. S_{50}, n and V_{max} values were 370μM, 1.8 and 1152pmol/min.mg, respectively. The S_{50} is approximately 25% lower than that observed for this pathway in the absence of co-expressed recombinant HSA (462μM). In contrast, the V_{max} and n values (1152pmol/min.mg and 1.8) for AZT glucuronidation in HEK293 cell lysates expressing both UGT2B7 and HSA was essentially identical to the values (1065pmol/min.mg and 1.6) for cells expressing UGT2B7 alone.

DISCUSSION

All forms of BSA increased the rate of AZT glucuronidation by both HLM and UGT2B7 in a concentration dependent manner, due to a decrease in K_m. A similar effect was observed with HSA-FAF, but 'crude' HSA exhibited a biphasic effect (decreased K_m at 0.1%, increased K_m at 2%) on AZT glucuronidation. There was also a trend to increasing K_m at higher concentrations of HSA-GF and HSA-FAFGF. Consistent with the effects on AZT glucuronidation, BSA and HSA-FAF, but not HSA, enhanced the rate of 4-MU glucuronidation due to a decrease in S_{50}. Similar data have been reported for the effects of different albumin preparations on CYP2C9 activity (Zhou *et al* 2004). These results led us to hypothesize that fatty acids present in, or released during, incubations acted as competitive inhibitors of UGT2B7 catalyzed AZT and 4-MU glucuronidation. We have demonstrated previously that unsaturated long chain fatty acids (oleic, linoleic and arachidonic) are potent inhibitors of UGT2B7 and UGT1A9 (Tsoutsikos *et al.* 2004). K_i values for linoleic and arachidonic acid inhibition of UGT2B7 were 6.3 and 0.15μM, respectively. By contrast, saturated and short- and medium- chain fatty acids minimally affect UGT activity (Tsoutsikos *et al.* 2004).

Analysis of the fatty acid content of HLM, HEK293 cell lysate, BSA, HSA and HSA-FAF was thus undertaken. Consistent with previous reports (Waskell *et al.* 1982; Kapitulnik *et al.* 1987), the unsaturated long chain fatty acid content of HLM was high, with oleic (C18:1), linoleic (C18:2) and arachidonic (C20:4) acids the most prevalent. The fatty acid content of HEK293 cell *lysate* was significantly (10-fold) lower. Oleic, linoleic and arachidonic acids were the most abundant unsaturated long chain fatty acids present in 'crude' HSA, whereas the content of these fatty acids in HSA-FAF and BSA was an order of magnitude lower. Oleic, linoleic and arachidonic acids, and other unsaturated and saturated long chain fatty acids (myristic (14:0), myristoleic (14:1), palmitic (16:0), palmitoleic (16:1), stearic (18:0), linolenic (18:3), arachidic

(20:0), eicosenoic (20:1), dihomo-linolenic (20:3) and eicosapentaenoic acids (20:5))
were all shown to be glucuronidated by UGT2B7. It has been demonstrated previously
that linoleic and arachidonic acids are substrates of UGT2B7 (Jude *et al.* 2001;
Turgeon *et al.* 2003; Little *et al.* 2004). Importantly, bands corresponding to the R_f
values of unsaturated long chain fatty acid glucuronides were observed in incubations
of HLM with ^{14}C-labelled UDPGA. The intensity of the bands was an order of
magnitude lower for HEK293 cells expressing UGT2B7. Addition of BSA and HSA-
FAF resulted in a concentration dependent reduction in the band intensity. In contrast,
the intensity of the putative FA glucuronide bands produced by incubations of HLM
with ^{14}C-labelled UDPGA increased in the presence of crude HSA.

Consistent with the postulated inhibitory effect of fatty acids on UGT2B7 activity,
addition of oleic, linoleic and arachidonic acids, individually and as a mixture, to
incubations of HEK293 cell lysate expressing UGT2B7 decreased both AZT and 4MU
glucuronidation activity, due to an increase in K_m (AZT) or S_{50} (4-MU) without a
change in V_{max}, indicative of a competitive mechanism. Addition of BSA and HSA-FAF
reversed the inhibition. The combined effect of oleic, linoleic and arachidonic acids
was similar to that of arachidonic acid alone. As noted previously, arachidonic acid is
the most potent fatty acid inhibitor of UGT2B7 identified to date (Tsoutsikos *et al.*
2004). Similar to the reversal of fatty inhibition observed with HSA-FAF, the K_m/S_{50}
values for AZT and 4MU glucuronidation were lower when UGT2B7 was co-
expressed with HSA, despite low HSA expression.

Whereas BSA (2%), BSA-FAF (2%) and HSA-FAF (2%) caused an approximate 10-
fold increase in the CL_{int} values for AZT glucuronidation by HLM and UGT2B7, the
increase in CL_{max} for 4-MU glucuronidation was somewhat lower (2- to 4- fold
increase). It should be noted that while CL_{int} and CL_{max} both represent *in vitro*
'clearances', the two parameters are not equivalent and are thus not directly

comparable (Houston and Kenworthy 2000). Nevertheless, the data demonstrate that unsaturated long chain fatty acids present in incubations influence the glucuronidation of UGT2B7 substrates that exhibit both 'classical' Michaelis Menten kinetics and positive homotropic cooperativity. Derived K_m values in previous studies have frequently been lower with recombinant UGT2B7 as the enzyme source compared to HLM. For example, K_m values for AZT, codeine, morphine (3- and 6-) and naproxen glucuronidation have variably been reported as 2- to 6-fold lower with recombinant UGT2B7, irrespective of whether the enzyme was expressed in a mammalian cell line (HEK293) or as 'baculosomes' (baculovirus-mediated expression) (Soars *et al.* 2002; Court *et al.* 2003; Uchaipichat *et al.* 2006). These observations are consistent with a lower content of inhibitory unsaturated long chain fatty acids in the expression systems.

Extrapolated 'whole liver' CL_{int} values, from scaling of microsomal data, typically under-predict the known hepatic clearance of UGT2B7 substrates (Boase and Miners 2002; Soars *et al.* 2002; Engtrakul *et al.* 2005; Riley *et al.* 2005). Despite the 10-fold higher CL_{int} values observed here for human liver microsomal AZT glucuronidation in the presence of BSA and HSA-FAF, predicted hepatic clearances (based on the approach of Uchaipichat *et al.* 2006) ranged from approximately 25 to 30 L/hr (cf-actual value of 87L/hr). Predicted AZT hepatic glucuronidation clearances of 41 and 63L/hr have been reported based on kinetic constants obtained with human hepatocytes (Naritomi *et al.* 2003; Engtrakul *et al.* 2005). Other studies have generally demonstrated improved predictivity of *in vivo* drug glucuronidation clearance using human hepatocytes (Soars *et al.* 2002; Riley *et al.* 2005), although a trend to under-prediction remains (Ito and Houston 2004; Miners *et al.* 2006). Notably, mean K_m values observed here for AZT glucuronidation by HLM (87-89μM) and recombinant UGT2B7 (40-52μM) in the presence of BSA and HSA-FAF were essentially identical to the K_m (87μM) for AZT glucuronidation by human hepatocytes reported by

Engtrakul *et al.* (2005), which correctly predicted AZT as a high hepatic clearance drug. Since there is no evidence of extrahepatic AZT metabolic clearance, the poorer predictivity of the human liver microsomal CL_{int} (in the presence of albumin) must arise from a lower V_{max}. The reason for the lower turnover by the microsomal enzyme is unclear, but may result from loss of active protein during HLM preparation, the presence of a non-competitive inhibitor in microsomal incubations, or limited substrate and/or cofactor access to the lumenally orientated enzyme (despite addition of the pore forming agent alamethicin). The V_{max} values observed here for AZT glucuronidation by HLM are similar to those reported previously by this (Boase and Miners 2002; Uchaipichat *et al.* 2006) and other (Court *et al.* 2003; Engtrakul *et al.* 2005) laboratories.

The formation of fatty acid glucuronides during incubations of HLM with UDPGA indicates that fatty acids present in the microsomal membrane (as phospholipids) are hydrolysed, presumably by the action of phospholipases, and released during the course of an incubation. It should be noted that dialysis of HLM against BSA in phosphate buffer did not change AZT glucuronidation kinetics (data not shown). Both BSA and HSA-FAF have the capacity to sequester inhibitory fatty acids, whereas fatty acid binding sites are presumably saturated in 'crude' HSA. It is also likely that 'crude' HSA contributes fatty acids to the incubation mixture, since fatty acids can desorb from binding sites on albumin despite high binding affinities (Hamilton 2002). Fatty acid glucuronide formation was enhanced for incubations conducted in the presence of HSA (Figure 4).

On the basis of improved predictivity of *in vivo* hepatic clearances from human hepatocyte kinetic data (i.e. CL_{int}), it has been suggested that HLM should not be used for predicting glucuronidation clearance or any kinetic parameters for metabolism or inhibition involving UGT enzymes (Engtrakul *et al.* 2005). Indeed,

based on the under-prediction generally observed using microsomal kinetic data, there appears to be a general preference for using human hepatocytes to assess drug metabolic stability (Naritomi *et al*. 2003; McGinnity *et al*. 2005; Riley *et al* 2005). Experimentally, however, HLM provide advantages over hepatocytes, particularly ease of use, decreased requirement for fresh tissue, and considerably lower cost. Previous results from this laboratory demonstrated that K_i values generated using HLM in the presence of BSA accurately predict the magnitude of inhibitory interactions involving glucuronidated drugs (Rowland *et al*. 2006; Uchaipichat *et al*. 2006). The present work similarly demonstrates that K_m values obtained with incubations of HLM and BSA / HSA-FAF are comparable to those observed with hepatocytes. Studies are in progress to further improve the predictivity of human liver microsomal kinetic data and characterise the universality of the 'albumin' effect with enzymes other than UGT2B7.

Based on reported K_m (and K_i) values for UGT substrates, there is a general perception that glucuronidation is a 'low affinity' metabolic pathway (for example; Williams *et al*., 2004). Data presented here suggest that previously reported K_m values for UGT2B7 substrates, and possibly those of other UGT enzymes, are over-estimated by up to an order of magnitude due to an experimental artefact. Reconsideration of current notions regarding the binding affinities of UGT substrates is clearly warranted.

JPET #118216

ACKNOWLEDGEMENTS

REFERENCES

Boase S, Miners JO (2002). *In vitro – in vivo* correlations for drugs eliminated by glucuronidation: investigation with the model substrate zidovudine. *Br J Clin Pharmacol*, 54: 493-503.

Bowalgaha K, Elliot DJ, Mackenzie PI, Knights KM, Swedmark S, Miners JO (2005). Naproxen and desmethylnaproxen glucuronidation by human liver microsomes and recombinant human UDP-glucuronosyltransferases (UGT): Role of UGT2B7 in the elimination of naproxen. *Br J Clin Pharmacol*, 60: 423-433.

Carlile DJ, Hakooz N, Bayliss MK, Houston JB (1999). Microsomal prediction of *in vivo* clearance of CYP2C9 substrates in humans. *Br J Clin Pharmacol*, 47: 625-635.

Court MH, Krishnaswamy S, Hoa Q, Duan SX, Patten CJ, von Moltke LL, Greenblatt DJ (2003). Evaluation of 3'-azido-3'-deoxymethymidine, morphine, and codeine as probe substrates for UDP-glucuronosyltransferase 2B7 (UGT2B7) in human liver microsomes: specificity and influence of the UGT2B7*2 polymorphism. *Drug Metab Dispos*, 31: 1125-1133.

Engtrakul JJ, Foti RS, Strelevitz TJ, Fisher MB (2005). Altered AZT (3'-azido-3'-deoxythymidine) glucuronidation kinetics in liver microsomes as an explanation for underprediction of in vivo clearance: comparison to hepatocytes and effect of incubation environment. *Drug Metab Dispos*, 33:1621-1627.

Folch J, Lees M, Stanley GHS (1956). A simple method for the isolation and purification of total lipids from animal tissue. *J Biol Chem*, 226: 497-509.

Griffin SJ, Houston JB (2004). Prediction of in vitro intrinsic clearance from hepatocytes: comparison of suspensions and monolayer cultures. *Drug Metab Dispos*, 33: 115-120.

Hamilton JA (2002). How fatty acids bind to proteins: the inside story from protein structures. *Prostaglandins Leukot Esset Fatty Acids*, 67: 65-72.

Houston JB (1994). Utility of in vitro drug metabolism data in predicting in vivo metabolic clearance. *Biochem Pharmacol*, 47: 1469–1479.

Houston JB, Kenworthy KE (2000). In vitro – in vivo scaling of CYP kinetic data not consistent with the classical Michaelis Menten model. *Drug Metab Dispos*, 28: 246-254.

Ito K, Iwatsubo T, Kanamitsu S, Nakajima, Sugiyama Y (1998). Quantitative prediction of in vivo drug clearance from in vitro data on metabolism, together with binding and transport. *Annu Rev Pharmacol Toxicol*, 38: 461-499.

Ito K, Houston JB (2004). Comparison of the use of liver models for predicting drug clearance using in vitro kinetic data from hepatic microsomes and isolated hepatocytes. *Pharm Res*, 21: 785-792.

Ito K, Houston JB (2005). Prediction of human drug clearance from in vitro and preclinical data using physiologically based and empirical approaches. *Pharm Res*, 22: 103-112.

Iwatsubo T, Hirota N, Ooie T, Suzuki H, Shimada N, Chiba K, Ishizaki T, Green CE, Tyson CA, Sugiyama Y (1997). Prediction of in vivo drug metabolism in the human liver from in vitro metabolism data. *Pharmacol Ther*, 73:147-171.

Jude AR, Little JM, Czernik PJ, Tephly TR, Grant DF, Radominska-Pandya (2001). Glucuronidation of linoleic acid diols by human microsomal and recombinant UDP-glucuronosyltransferases: Identification of UGT2B7 as the major isoforms involved. *Arch Biochem Biophys*, 389: 176-186.

Kapitulnik J, Weil E, Rabinowitz R, Krausz (1987). Fetal and adult human liver differ markedly in the fluidity and lipid composition of their microsomal membranes. *Hepatology*, 7: 55-60.

Little JM, Kurkela M, Sonka J, Jantti S, Ketola R, Bratton S, Finel M, Radominska-Pandya A (2004). Glucuronidation of oxidized fatty acids and prostaglandins B1 and E2 by human hepatic and recombinant UDP-glucuronosyltransferases. *J Lipid Res*, 45: 1694-1703.

Ludden LK, Ludden TM, Collins JM, Pentikis HS, Strong JM (1997). Effect of albumin on estimations, *in vitro*, of phenytoin Vmax and Km values; implications for clinical correlation. *J Pharmacol Exp Ther*, 282: 391-396.

McGinnity DF, Soars MG, Urbanowicz RA, Riley RJ (2005). Evaluation of fresh and cryopreserved hepatocytes as in vitro drug metabolism tools for the prediction of metabolic clearance. *Drug Metab Dispos*, 32: 1247-1253.

McLure JA, Miners JO, Birkett DJ (2000). Non-specific binding of drugs to human liver microsomes. *Br J Clin Pharmacol*, 49: 453-461.

Miners JO, Smith PA, Sorich MJ, McKinnon RA, Mackenzie PI (2004). Predicting human drug glucuronidation parameters: application of *in vitro* and *in silico* modeling approaches. *Annu Rev Pharmacol Toxicol*, 44: 1-25.

Miners JO, Knights KM, Houston JB, Mackenzie PI (2006). In vitro-in vivo correlation for drugs and other compounds eliminated by glucuronidation in humans: pitfalls and promises. *Biochem Pharmacol*, 71: 1531-1539.

Mistry M, Houston JB (1987). Glucuronidation in vitro and in vivo. Comparison of intestinal and hepatic conjugation of morphine, naloxone, and buprenorphine. *Drug Metab Dispos,* 15: 710-717.

Naritomi Y, Terashita S, Kagayama A, Sugiyama Y (2003). Utility of hepatocytes in predicting drug metabolism: comparison of hepatic intrinsic clearance in rats and humans in vivo and in vitro. *Drug Metab Dispos*, 31: 580-588.

Proctor NJ, Tucker GT, Rostami-Hodjegan A (2004). Predicting drug clearance from recombinantly expressed CYPs: intersystem extrapolation factors. *Xenobiotica*, 34: 151-178.

Riley RJ, McGinnity DF, Austin RP (2005). A unified model for predicting human hepatic, metabolic clearance from in vitro intrinsic clearance data in hepatocytes and microsomes. *Drug Metab Dispos*, 33: 1304-1311.

Rowland A, Elliot DJ, Williams JA, Mackenzie PI, Dickinson RG, Miners JO (2006). In vitro characterization of lamotrigine N2-glucuronidation and the lamotrigine-valproic acid interaction. *Drug Metab Dispos*, 34: 1055-1062.

Soars MG, Burchell B, Riley RJ (2002). *In vitro* analysis of human drug glucuronidation and prediction of *in vivo* metabolic clearance. *J Pharmacol Exp Ther*, 301: 382-390.

Stone AN, Mackenzie PI, Galetin A, Houston JB, Miners JO (2003). Isoform selectivity and kinetics of morphine 3- and 6-glucuronidation by human UDP-Glucuronosyltransferases: evidence for atypical glucuronidation kinetics by UGT2B7. *Drug Metab Dispos*, 31: 1086-1089.

Tang C, Lin Y, Rodrigues AD, Lin JH (2002). Effect of albumin on phenytoin and tolbutamide metabolism in human liver microsomes: an impact more than protein binding. *Drug Metab Dispos*, 30: 648-654.

Tsoutsikos P, Miners JO, Stapleton A, Thomas A, Sallustio BC, Knights KM (2004). Evidence that unsaturated fatty acids are potent inhibitors of renal UDP-glucuronosyltransferases (UGT): kinetic studies using human kidney cortical microsomes and recombinant UGT1A9 and UGT2B7. *Biochem Pharmacol*, 67: 191-199.

Turgeon D, Chouinard S, Belanger P, Picard S, Labbe JF, Borgeat P, Belanger A (2003). Glucuronidation of arachidonic and linoleic acid metabolites by human UDP-glucuronosyltransferases. *J Lipid Res*, 44: 1182-1190.

Uchaipichat V, Mackenzie PI, Guo XH, Gardner-Stephen D, Galetin A, Houston JB, Miners JO (2004). Human UDP-Glucuronosyltransferases: isoform selectivity and kinetics of 4-methylumbelliferone and 1-napthol glucuronidation, effects of organic

solvents, and inhibition by diclofenac and probenecid. *Drug Metab Dispos*, 32: 413-423.

Uchaipichat V, Winner LK, Mackenzie PI, Elliot DJ, Williams JA, Miners JO (2006). Quantitative prediction of *in vivo* inhibitory drug interactions involving glucuronidated drugs from *in vitro* data: The effect of fluconazole on zidovudine glucuronidation. *Br J Clin Pharmacol*, 61: 427-439.

von Moltke LL, Greenblatt DJ, Schmider J, Wright CE, Harmatz JS, Shader RI (1998). In vitro approaches for predicting drug interactions in vivo. *Biochem Pharmacol*, 55: 113-122.

Wang JS, Wen X, Backman JT, Neuvonen PJ (2002). Effect of albumin and cytosol on enzyme kinetics of tolbutamide hydroxylation and on inhibition of CYP2C9 by gemfibrozil in human liver microsomes. *J Pharmacol Exp Ther*, 302: 43-49.

Ward KW (2005). Recent advances in pharmacokinetic extrapolation from preclinical data to humans. *Expert Opin Drug Metab Toxicol*, 1: 583-594.

Waskell L, Koblin D, Canova-Davis E (1982). The lipid composition of human liver microsomes. *Lipids*, 17: 317-320.

Wienkers LC, Heath TG (2005). Predicting in vivo drug interactions from in vitro drug discovery data. *Nat Rev Drug Discov*, 4: 825-833.

Williams JA, Hyland R, Jones BC, Smith DA, Hurst S, Goosen TC, Peterkin V, Koup JR, Ball SE (2004) Drug-drug interactions for UDP-glucuronosyltransferase

substrates: A pharmacokinetic explanation for typically observed low exposure (AUCi/AUC) ratios. *Drug Metab Disp* 32: 1201-1208.

Zhou Q, Matsumoto S, Ding LR, Fischer NE, Inaba T (2004). The comparative interaction of human and bovine serum albumins with CYP2C9 in human liver microsomes. *Life Sci*, 75: 2145-2155.

JPET #118216

FOOTNOTES

LEGENDS FOR FIGURES

Figure 1. Effect of crude and modified (fatty acid free (FAF), globulin free (GF) and combined fatty acid and globulin free (FAF-GF)) forms of bovine and human serum albumins on the rate of AZT glucuronidation by HLM and recombinant UGT2B7. Each bar represents the mean of duplicate estimations.

Figure 2. Representative velocity versus substrate concentration plots for AZT glucuronidation by human liver microsomes (HLM), in the presence of bovine serum albumin (BSA), human serum albumin (HSA) and fatty acid free HSA (HSA-FAF). (Sets of kinetic curves were generated on four separate occasions; see Tables 1 and 2 for mean kinetic constants.) Points are experimentally determined values, while curves are from model – fitting.

Figure 3. TLC autoradiogram showing the formation of fatty acid glucuronides by recombinant UGT2B7. Abbreviations: myristic (14:0), myristoleic (14:1), palmitic (16:0), palmitoleic (16:1), stearic (18:0), oleic (18:1), linoleic (18:2), linolenic (18:3), arachidic (20:0), eicosenoic (20:1), dihomo-linolenic (20:3), arachidonic (20:4) and eicosapentaenoic acids (20:5).

Figure 4. TLC autoradiogram showing the formation of fatty acid glucuronides by incubations of human liver microsomes (HLM) and recombinant UGT2B7 with ^{14}C-UDPGA, conducted in the presence and absence of crude bovine serum albumin (BSA) and crude (HSA) and fatty acid free (HSA-FAF) forms of human serum albumin. Formation of the glucuronides of exogenous linoleic and arachidonic acids (with HLM as the enzyme source) is shown for comparison, along with the R_f of a xenobiotic substrate (4MU).

Figure 5. Immunoblot analysis of human serum albumin (HSA) expression by HEK293 cells co-transfected with UGT2B7 and HSA cDNAs. Abbreviations: NC, negative control (HEK293 cells transfected with UGT2B7 alone); C-T, co-transfected cells (HEK293 cells co-transfected with HSA and UGT2B7).

Table 1 - Effect of bovine serum albumin preparations on the kinetics of zidovudine glucuronidation by human liver microsomes and recombinant UGT2B7

enzyme source	parameter	no albumin	crude		FAF		GF		FAF-GF	
			0.5%	2.0%	0.5%	2.0%	0.5%	2.0%	0.5%	2.0%
HLM	K_m	1113 ± 56	105 ± 6*	87 ± 2*	124 ± 3*	125 ± 14*	211 ± 12*	188 ± 4*	135 ± 6*	136 ± 6*
	V_{max}	738 ± 13	746 ± 27	867 ± 40	859 ± 6	785 ± 19	755 ± 34	715 ± 54	810 ± 44	900 ± 10
	CL_{int}	0.66	7.11	9.97	6.93	6.28	3.58	3.80	6.02	6.62
UGT2B7	K_m	439	75	40	75	44	95	97	102	99
	V_{max}	50	43	56	48	56	47	48	45	46
	CL_{int}	0.113	0.569	1.408	0.642	1.272	0.498	0.491	0.445	0.463

Data for HLM are the mean ± SD of four replicates, while data for UGT2B7 represent the mean of duplicate experiments.

Units: K_m, μM; V_{max}, pmol/min.mg; CL_{int}, μL/min.mg.

Abbreviations for albumin (BSA) preparations: FAF, essentially fatty acid free; GF, essentially globulin free; FAF-GF, essentially fatty acid and globulin free. 'Crude' refers to unmodified BSA.

* $p < 0.05$ compared to incubations conducted without albumin.

Table 2 - Effect of human serum albumin preparations on the kinetics of zidovudine glucuronidation by human liver microsomes and recombinant UGT2B7

enzyme source	parameter	no albumin	Crude		FAF		GF		FAF-GF	
			0.1%	2.0%	0.1%	2.0%	0.1%	2.0%	0.1%	2.0%
HLM	K_m	1113 ± 56	374 ± 16*	1575 ± 69	123 ± 1*	89 ± 4*	119 ± 3*	233 ± 13*	172 ± 6*	422 ± 7*
	V_{max}	738 ± 13	893 ± 22	810 ± 59	751 ± 15	699 ± 8	725 ± 7	809 ± 18	565 ± 13	673 ± 13
	CL_{int}	0.663	2.39	0.514	6.10	7.88	6.11	3.48	3.28	1.60
UGT2B7	K_m	439	373	891	94	52	131	165	156	258
	V_{max}	50	48	39	43	47	49	42	40	43
	CL_{int}	0.113	0.129	0.043	0.451	0.899	0.371	0.254	0.258	0.168

Data for HLM are the mean ± SD of four replicates, while data for UGT2B7 represent the mean of duplicate experiments.

Units: K_m, μM; V_{max}, pmol/min.mg; CL_{int}, μL/min.mg.

Abbreviations for albumin (HSA) preparations: FAF, essentially fatty acid free; GF, essentially globulin free; FAF-GF, essentially fatty acid and globulin free. 'Crude' refers to unmodified HSA.

* $p < 0.05$ compared to incubations conducted without albumin.

40

Table 3 - Effects of albumin preparations on the kinetics of 4-methylumbelliferone glucuronidation by recombinant UGT2B7

parameter	no albumin	BSA			HSA			HSA-FAF		
		0.1%	1.0%	2.0%	0.1%	1.0%	2.0%	0.1%	1.0%	2.0%
S_{50}	462	311	246	213	432	375	426	314	164	102
n	1.6	1.5	1.6	1.6	1.5	1.7	1.5	1.6	1.7	2.1
V_{max}	1065	1115	1140	1195	1221	848	990	1329	1226	1093
CL_{max}	2.31	3.58	4.63	5.61	2.82	2.26	2.32	4.23	7.47	10.71

Data represent the mean of duplicate estimations.

Units: K_m, µM; V_{max}, pmol/min.mg; CL_{max}, L/hr (calculated according to equation 1, *Data analysis*).

Abbreviations for albumin preparations: BSA, unmodified (or 'crude') bovine serum albumin; HSA, unmodified (or 'crude') human serum albumin; HSA-FAF, essentially fatty acid free HSA.

41

Table 4 – Content of C16 to C20 series fatty acids in human liver microsomes, HEK293 cell lysate and albumin preparations

[Fatty Acid]	HEK293	HLM	BSA	HSA	HSA-FAF
16:0	6.64	51.1	4.69	58.3	9.28
16:1n-9	0.56	1.71	0.03	0.91	0.11
16:1n-7	1.29	12.8	0.38	4.67	0.38
16:2n-3	0.06	0.34	0.03	0.18	0.02
18:0	3.16	62.6	3.50	17.9	4.72
18:1n-9	7.76	67.3	3.47	46.2	3.77
18:1n-7	1.57	7.36	0.48	3.84	0.44
18:2n-9	0.02	0.52	0.03	0.37	0.03
18:2n-6	0.90	65.3	2.74	42.0	8.40
18:3n-6	0.03	1.01	0.02	0.45	0.05
18:3n-3	0.03	0.77	0.10	2.07	0.08
20:0	0.12	0.37	0.04	0.13	0.05
20:1n-11	0.04	0.11	0.00	0.09	0.00
20:1n-9	0.27	0.52	0.00	0.33	0.05
20:2n-9	0.03	0.13	0.00	0.10	0.01
20:2n-6	0.04	0.70	0.00	0.33	0.07
20:3n-9	0.11	0.62	0.00	0.13	0.04
20:3n-6	0.27	6.12	0.05	1.10	0.71
20:4n-6	1.13	32.9	0.07	5.58	2.98
20:3n-3	0.02	0.19	0.00	0.07	0.03

Units: [fatty acid], µM for a 1 mg/ml suspension of HLM, HEK293 cell lysate and 2% solutions (20 mg/ml) of albumin preparations.

42

Table 5 - Effect of albumin preparations on the inhibition of AZT glucuronidation by fatty acids with recombinant UGT2B7 as the enzyme source

Albumin Preparation	18.1n-9 concentration	Rate of GAZT formation	18.2n-6 concentration	Rate of GAZT formation	20.4n-6 concentration	Rate of GAZT formation	FAM[a] concentration	Rate of GAZT formation
None	0	19.6	0	19.6	0	19.6	0	19.6
	3	15.0	3	13.3	1.5	8.1	7.5	10.4
BSA	0	38.3	0	38.3	0	38.3	0	38.3
	3	37.4	3	38.3	1.5	36.8	7.5	38.7
HSA-FAF	0	31.3	0	31.3	0	31.3	0	31.3
	3	31.3	3	32.4	1.5	31.2	7.5	31.6

Incubations were conducted with AZT (400 µM) as substrate, ± albumin and ± fatty acids. Data represent mean of duplicate estimations.

Units: [fatty acid], µM; rate of GAZT formation, pmol/min.mg.

Abbreviations for albumin preparations: BSA, unmodified (or 'crude') bovine serum albumin; HSA-FAF, essentially fatty acid free human serum albumin.

[a] FAM: Fatty acid mixture comprising oleic (18.1n-9), linoleic (18.2n-6) and arachidonic (20.4n-6) acids; individual concentrations were 3µM 18.1n-9, 3µM 18.2n-6 and 1.5µM 20.4n-6.
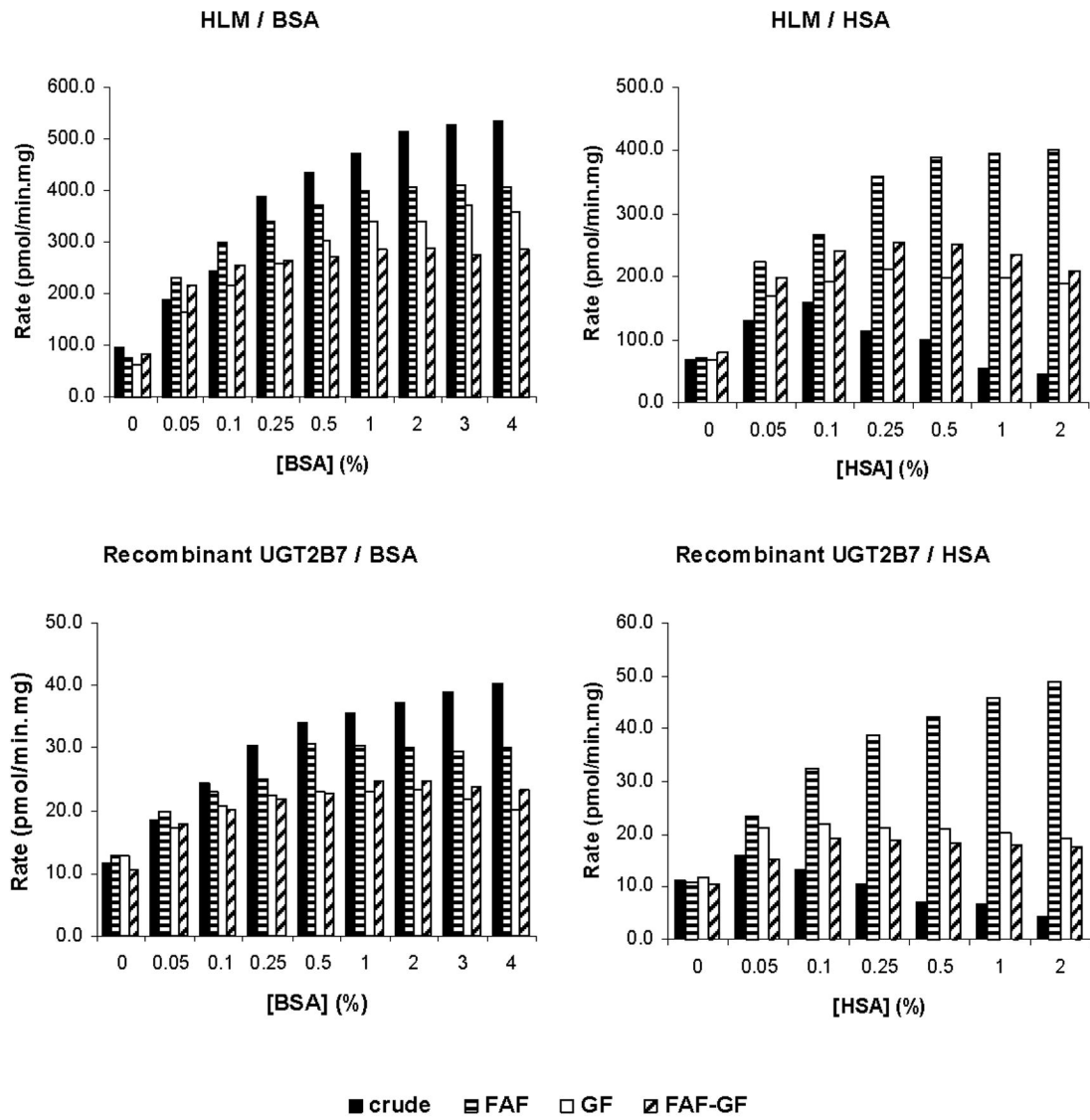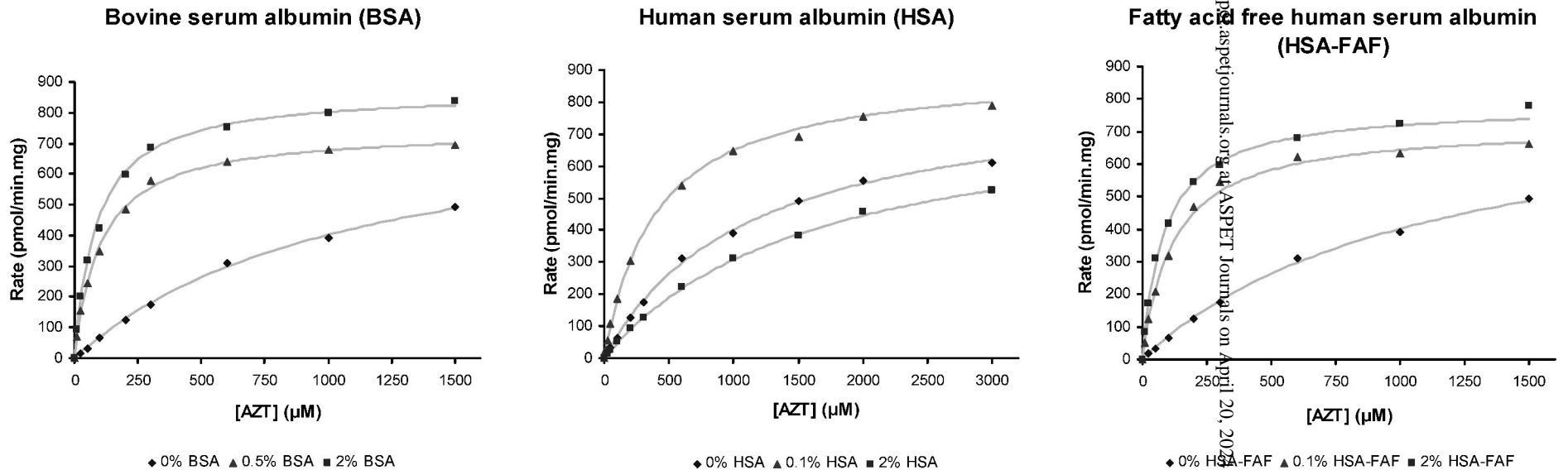
43

Figure 1

HLM / BSA

HLM / HSA

Recombinant UGT2B7 / BSA

Recombinant UGT2B7 / HSA

■ crude   ⊟ FAF   □ GF   ▨ FAF-GF

Figure 2

Bovine serum albumin (BSA)

Human serum albumin (HSA)

Fatty acid free human serum albumin (HSA-FAF)

Figure 3

Figure 4

HLM with arachidonic acid

HLM with linoleic acid

HLM

HLM with 0.1% HSA

HLM with 1% HSA

HLM with 2% HSA

HLM with 0.1% HSA-FAF

HLM with 2% HSA-FAF

HLM with 0.1% BSA

HLM with 2% BSA

HLM with 4MU

Figure 5

60kDa -

NC   C-T   C-T   10ng 20ng 50ng 100ng

HSA standards